A COMPARATIVE STUDY ON THE PREPARATION OF GLASSY CARBON ELECTRODES MODIFIED WITH ELECTROCHEMICALLY REDUCED GRAPHENE OXIDE

Andra Mihaela ONAȘ[1], Elena OLARET[2], Andreea Madalina PANDELE[3], Matei RAICOPOL[4*], Luisa PILAN[5*], Horia IOVU[6*]

This work introduces a novel comparative analysis on the morphology, surface chemistry and electrochemical behavior of electrochemically reduced graphene oxide (ERGO) modified electrodes obtained by two commonly used methods: direct electrodeposition, and electrochemical reduction of GO drop-casted films. We report that electrodes modified through drop-casting are uniformly coated with ERGO layers, unlike electrodes obtained through electrodeposition, which only show isolated ERGO agglomerates on their surface. However, cyclic voltammetry investigations in the presence of soluble redox probes indicate that drop-casting is less reproducible for producing ERGO-modified electrodes, evidenced by 17-fold increase in the relative standard deviation of the estimated surface area.

Keywords: modified glassy carbon electrodes, electrochemically reduced graphene oxide, drop casting, electrodeposition, surface analysis

1. Introduction

Glassy carbon (GC) is a carbonaceous material produced by the slow thermal degradation of certain cured polymeric resins. This material exhibits interesting properties, the ones particularly significant for the electrochemical field being its high chemical resistance and its very low electrical resistivity ($3 \cdot 10^{-4}$ to $8 \cdot 10^{-4}$ Ω·cm) [1,2]. These attributes have recommended GC as a promising alternative for conventional metallic electrodes. The first works reporting the use of GC electrodes date back to 1965 [3,4] and since then there have been numerous

[1] PhD student, Advanced Polymer Materials Group, University POLITEHNICA of Bucharest, Romania, e-mail: andra_mihaela.onas@upb.ro
[2] PhD student, Advanced Polymer Materials Group, University POLITEHNICA of Bucharest, Romania, e-mail: elena.olaret@upb.ro
[3] Assoc. Prof., Advanced Polymer Materials Group, University POLITEHNICA of Bucharest, Romania, e-mail: pandele.m.a@gmail.com
[*4] Assoc. Prof, Faculty of Chemical Engineering and Biotechnologies, University POLITEHNICA of Bucharest, Romania, corresponding author, e-mail: m_raicopol@chim.upb.ro
[*5] Prof., Faculty of Chemical Engineering and Biotechnologies, University POLITEHNICA of Bucharest, Romania, corresponding author, e-mail: luisa.pilan@upb.ro
[*6] Prof., Advanced Polymer Materials Group, University POLITEHNICA of Bucharest, Romania, corresponding author, e-mail: horia.iovu@upb.ro

studies that demonstrate the successful use of GC electrodes for electrochemical detection [5,6], biosensing [7,8], diagnostics [9,10] or other high-end applications.

Different strategies for the surface modification of GC electrodes were proposed in order to improve detection sensitivity in various electroanalytical applications. Among these strategies, modifying the GC surface with carbon nanomaterials, such as graphene and its variants (CVD graphene, graphene oxide, reduced graphene oxide, etc.) has attracted significant interest for electrochemical biosensing applications, owing to their outstanding structural and electronic characteristics, including high mechanical strength, large surface area, and exceptional conductivity [11–13]. Graphene oxide (GO) is a two-dimensional nanomaterial composed of single graphitic layers which contain various oxygenated groups like carboxyl, epoxy, or hydroxyl [14,15]. Reduced graphene oxide (RGO) has demonstrated several advantages over GO or pristine graphene in electroanalytical applications. The oxygenated functional groups and the defects present on the surface of RGO sheets can enhance the electrocatalytic activity and enable further modifications [16]. Electrochemical reduction of GO is one of the most powerful reduction techniques, as it does not involve the use of toxic reagents, and the reduced GO does not contain impurities associated with the use of reducing agents. Furthermore, the electrochemical reduction process can be very well controlled by adjusting the applied potential, leading to electrochemically reduced GO (ERGO) with tailorable oxygenated groups composition [16]. In ERGO, the majority of oxygen-containing groups of the initial GO are gradually removed upon reduction, restoring the sp^2 carbon lattice. Thus, π-π interactions between stacked ERGO sheets and between sheets and the GC substrate are enhanced, promoting electron transfer and electrical conductivity [17].

There are two commonly employed methods for obtaining ERGO-modified electrodes: either the direct electrochemical reduction of GO at the bare substrate electrode or the electrochemical reduction of a pre-deposited GO film, often referred to as the "drop-casting" method [16]. In the first case, the working electrode is immersed in a GO suspension containing a supporting electrolyte, and by applying a sufficient negative potential, ERGO is directly deposited onto the electrode surface [18]. The drop-casting method comprises several steps, starting with the deposition of a GO suspension onto the surface of the working electrode, followed by drying, and ultimately, the electrochemical reduction of the deposited GO in an electrolyte solution [19]. Both methods offer the possibility to modify GC substrates with ERGO, but a comparison of modified electrodes obtained by the two approaches has not been reported to date. The choice of the most suitable approach for electrode modification is an important step in electrochemical sensing platform fabrication, and it might prove crucial for device performance. In this context, our work provides a comparative analysis of the obtained ERGO layers in terms of surface morphology, surface chemistry and electrochemical properties.

2. Experimental

2.1. Reagents and materials

Graphene oxide (in form of 2 mg/mL dispersion in H_2O), Na_2CO_3, $NaHCO_3$, KCl, HNa_2PO_4, H_2NaPO_4, as well as acetonitrile (MeCN, anhydrous, 99.9%) were supplied by Sigma-Aldrich. Tetrabutylammonium tetrafluoroborate ($TBABF_4$, electrochemical grade, 99%) was purchased from Fluka Analytical, while $K_3[Fe(CN)_6]$, $K_4[Fe(CN)_6]\cdot 3H_2O$, and ferrocene (98%) were received from Merck. All chemicals were used in their original, as-received state, and ultrapure water (18.2 MΩ·cm) was used for the preparation of the aqueous solutions.

2.2. Electrode modification procedures

Before modification, the GC electrodes were polished using a 0.05 μm alumina suspension (Akasel) on a microfiber pad (Aka-Napal, Akasel) for 1 minute (2 × 30 s), followed by an ultrasonication treatment in UPW for 6 minutes (2 × 3 min), and then kept in water before use. After polishing, the electrodes were tested by running one cyclic voltammetry (CV) cycle at a scan rate of 0.1 V s^{-1}, in the presence of $K_3[Fe(CN)_6]$ redox probe (1mM, in 0.1M KCl electrolyte solution), to ensure their correct surface cleaning ($\Delta E_p < 0.07$ V).

The procedure employed for the ERGO preparation via the direct electrochemical reduction of GO on GC electrodes was adapted from a protocol described by Chen et al [18]. The deposition process was performed in a degassed (argon, 15 min), 0.2 mg mL^{-1} aqueous dispersion of GO in carbonate/bicarbonate buffer (0.05 M, pH = 9.2), under magnetic stirring. The electroreduction process involved 10 CV cycles in the potential range 0.5 to −1.4 V vs SCE, at a scan rate of 0.05 V s^{-1}. The modified electrodes fabricated by this procedure were rinsed with ultrapure water, air dried and deposited in sealed containers before further use, and have been denoted GC_ERGO(ed).

The ERGO preparation by the drop-casting procedure was adapted from the method employed by Guo et al [19]. A volume of 6.5 μL GO dispersion (0.05 mg mL^{-1}) was casted on the freshly polished GC electrode surface, and then air-dried at room temperature. The resulting GO-modified electrodes were subsequently subjected to electrochemical reduction by CV. Degassed phosphate buffer (50 mM, pH 6) was used as electrolyte, and the reduction was performed for 10 CV cycles ranging from 0 to −1.7 V vs SCE, at 0.05 V s^{-1}. After electrochemical reduction, the electrodes were rinsed with ultrapure water, air dried and deposited in sealed containers before further use. The modified electrodes obtained by this two steps methodology have been further denoted GC_GO(dc) and GC_ERGO(dc), respectively.

2.3. Instrumentation

Optical microscopy images were revealed using a Carl Zeiss Technival 2 stereomicroscope and a Carl Zeiss Epival microscope equipped for differential interference contrast imaging in reflected light. The images from atomic force microscopy were captured using the AFM tapping mode of a NeaSNOM microscope. The displayed figures show a 5.0 μm × 5.0 μm surface area.

X-ray photoelectron spectroscopy measurements were acquired using a K-Alpha spectrometer (Thermo Scientific) outfitted with an Al Kα monochromatic source (1486.6 eV). A flood gun was employed for compensating the charging effects, while binding energies were calibrated internally by shifting the main C1s peak to 284.8 eV. C1s deconvolutions were performed after subtracting a Shirley background.

A Renishaw inVia Raman microscope, equipped with a 473nm excitation laser, was employed for recording the Raman spectra, using a 10× objective and three accumulations for the acquisition of each spectrum.

Electrochemical experiments were carried out at room temperature (~25 ^{o}C), using a Metrohm Autolab 128N potentiostat, and employing a conventional three-electrode configuration. The bare or modified GC electrodes (disks, 3 mm diameter, ALS Co. Ltd. Tokyo, Japan) were used as working electrodes, and a platinum rod as counter electrode. For the aqueous solutions studies either Ag/AgCl, KCl (sat.) or a saturated calomel electrode (SCE) served as reference electrodes, while Ag/10 mM Ag^{+}, 0.1M $TBABF_4$, in MeCN reference was employed in non-aqueous solutions. The electrodes subjected to XPS and Raman analysis were GC disks with a diameter of 6 mm (OrigaLys, France).

3. Results and Discussion

3.1. Preparation of Modified Electrodes

Fig. 1 displays typical successive CVs recorded during the preparation of GC_ERGO electrodes by the two methodologies. In the both cases, the first potential cycle displays an easily discernible irreversible peak around the potential of −1 V, corresponding to the reduction of the oxygen-containing groups of GO [18,19]. For GC_ERGO(ed) preparation, the gradual deposition of the conductive ERGO onto the GC electrode for each potential scan is confirmed by the increase of the peak and capacitive currents. Additionally, the pair of redox peaks appearing around 0 ÷ 0.2 V is generally associated with more stable electrochemically active oxygenated groups present on the surface of graphene [18,20]. For the second preparation procedure, the cathodic peak appearing in the first reduction cycle at a potential close to −1 V is much larger, having an onset potential of approximately −0.6 V. This peak disappears in the following cycles or is displaced at more negative potentials [21]. After 10 cycles the reduction currents decrease

considerably, proving the irreversible electrochemical reduction of the oxygen-containing functional groups of GO at negative potentials [19].

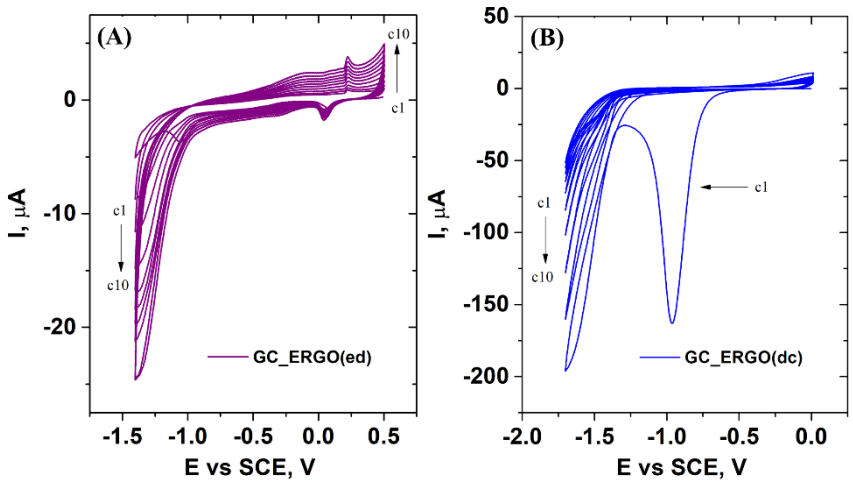

Fig. 1. Typical CVs (0.05 Vs^{-1}, 10 cycles) for the GC_ERGO electrodes preparation by the two strategies: (A) direct electrochemical reduction of GO at GC electrodes from a deaerated 0.2 mg mL^{-1} GO dispersion in 50 mM carbonate buffer, pH 9.2, under magnetic stirring, and (B) the electrochemical reduction of drop-coated GO onto GC electrodes in a deareated 50mM phosphate buffer, pH 6.

3.2. Characterization of Modified Electrodes

3.2.1. Surface morphology

The ERGO electrodes' surface was investigated after each modification step using optical microscopy (Fig. 2). While the image of the GC_ERGO(ed) sample reveals only small agglomerates of ERGO on the electrode surface, the GC_GO(dc) and GC_ERGO(dc) samples are covered by continuous graphene films. The micrographs obtained with differential interferential contrast in reflected light reveal the uneven characteristic of the GO drop-casted layer, as indicated by various interference colors that appear due to surface height differences. On the contrary, the electrode surface becomes very smooth after the electrochemical reduction step is performed.

The surface topography was examined using AFM, and the micrographs are presented in Fig. 3.

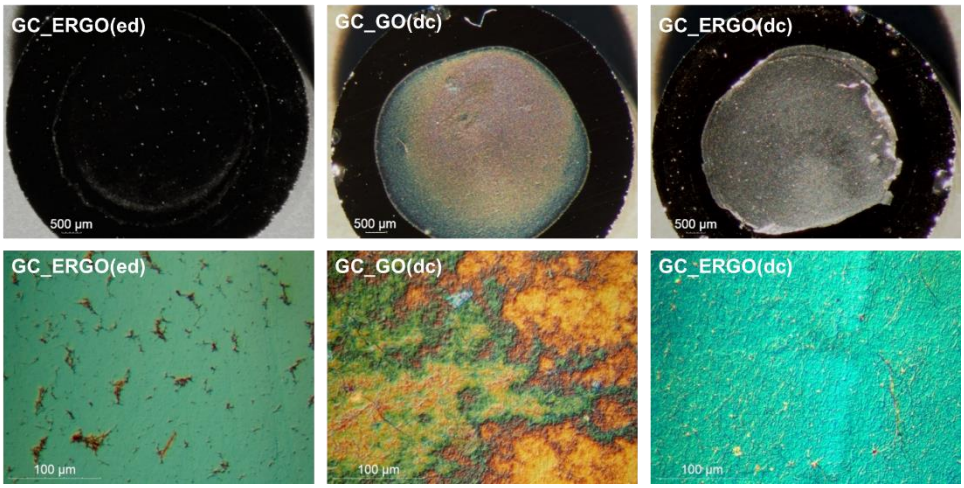

Fig. 2. Optical images showing the GC modified electrodes surface appearance (top) and the graphene deposit microstructure using differential interferential contrast in reflected light (bottom).

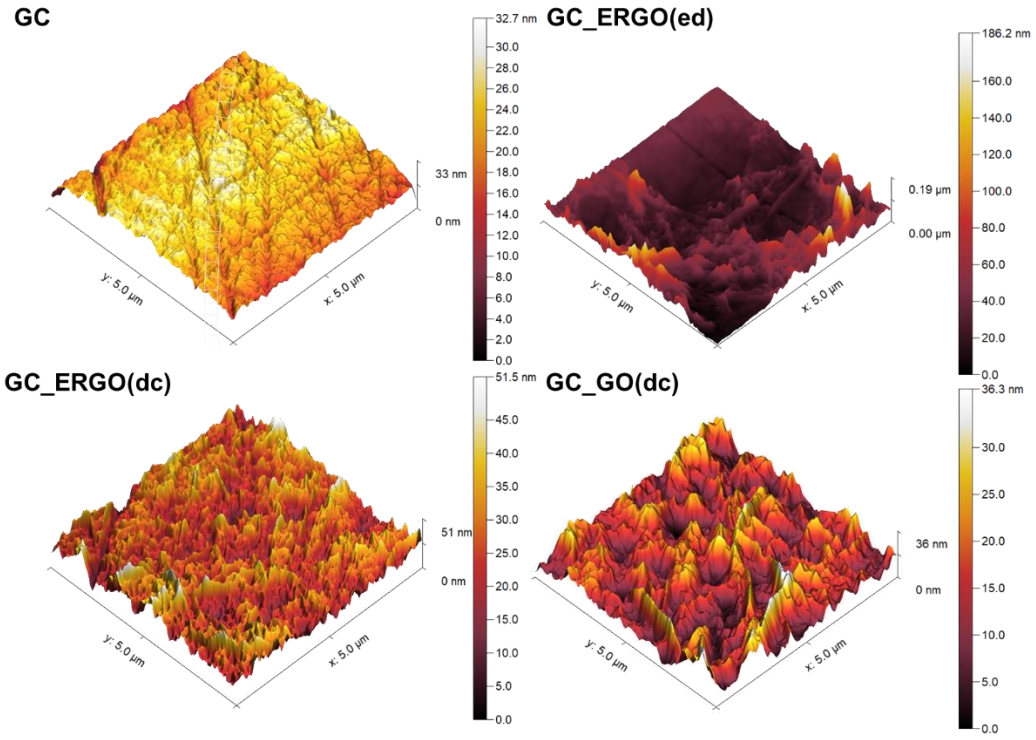

Fig. 3. AFM micrographs showing surface morphology for selected areas of the bare GC, and the modified electrodes GC_ERGO(ed), GC_GO(dc) and GC_ERGO(dc).

Similarly to the results obtained using optical microscopy, the AFM images of the GC_ERGO(ed) surface show the formation of uneven ERGO agglomerates

which do not cover the entire electrode surface. While the GC_GO(dc) sample exhibits an increased rugosity, the GC_ERGO(dc) sample has a roughness closer to the bare GC substrate, which suggests the formation of tightly packed ERGO layers on the electrode surface.

3.2.3. X-ray Photoelectron Spectroscopy

The surface chemical composition of the electrodeposited layers was further assessed by XPS. Fig. 4 depicts the XPS survey spectra for the analyzed surfaces. The GC_GO(dc) sample has an increased oxygen content, indicating the abundance of various oxygen-containing functionalities. The ERGO samples have a similar atomic composition, but with a lower oxygen content, confirming the partial reduction of oxygen functionalities.

Fig. 5 shows the corresponding C1s core-level spectra for the tested samples, which were deconvoluted into several components. The characteristic peak at ~284.8 eV is associated with C atoms from graphitic domains [22], and peaks at 285.5, 287 and 288.5 eV correspond to carbon atoms from C-O and C-O-C bonds respectively, as depicted in Fig. 5. As expected, the GC_GO(dc) sample has the highest content of oxygenated groups, which decreases significantly after the electrochemical reduction step. Only the C-O-C and C-OH components are still visible in the GC_ERGO(dc) spectrum, confirming the successful reduction of drop-casted GO.

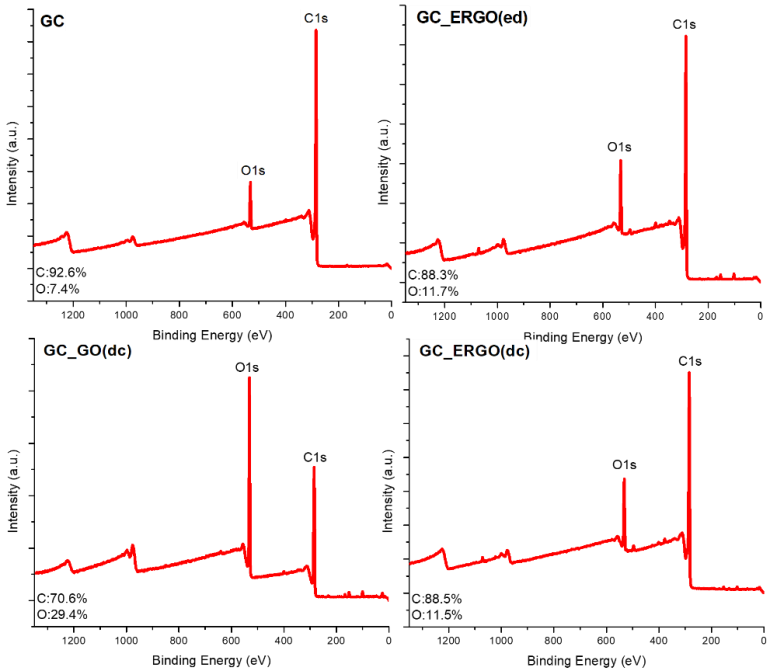

Fig. 4. XPS survey spectra for the bare GC substrate, and the modified electrodes GC_ERGO(ed), GC_GO(dc) and GC_ERGO(dc).

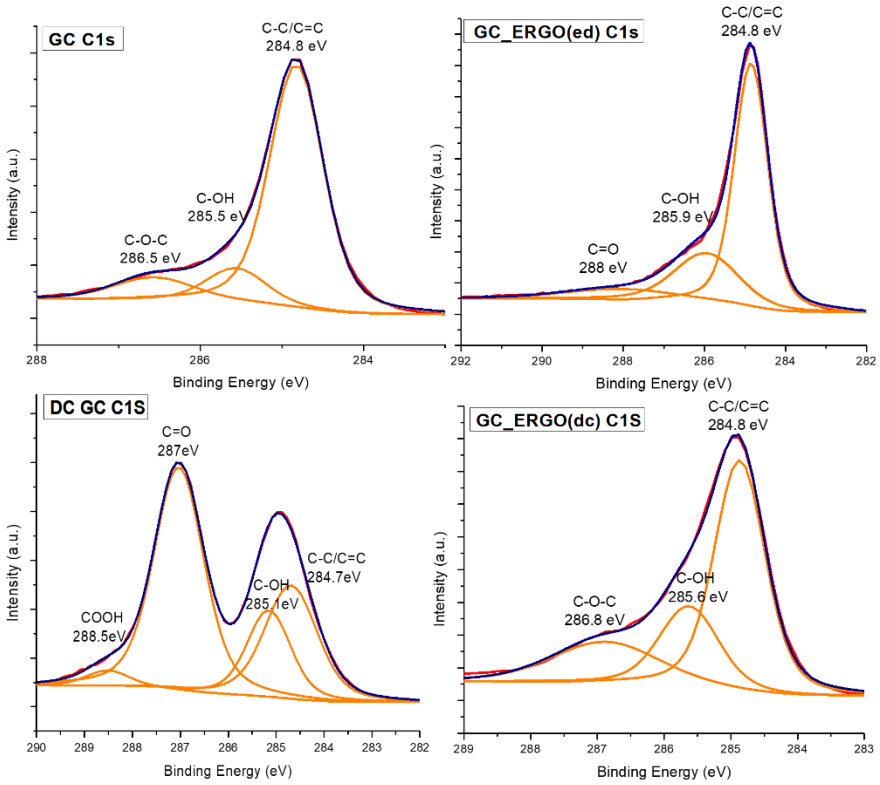

Fig. 5. XPS C1s deconvoluted spectra for the bare GC substrate, and the modified electrodes GC_ERGO(ed), GC_GO(dc) and GC_ERGO(dc)

3.2.4. Raman Spectroscopy

The Raman spectra for pristine GC and ERGO-modified GC substrates are presented in Fig. 6. The spectrum corresponding to the unmodified GC substrate is similar to previously reported Raman data [23], and shows the characteristic D and G bands with the accompanying 2D and D+G overtones. The obvious resemblance between the GC and GC_ERGO(ed) samples may be attributed to the incomplete surface coverage with small few-layer ERGO deposits. This is also supported by the 2D overtone still present in the GO_ERGO(ed) sample, which has been reported to indicate the formation of few-layered graphene aggregates [24]. As expected, the GC_GO(dc) and GC_ERGO(dc) samples display broad D and G peaks, indicating a high density of structural defects such as lattice vacancies and sp^3 C atoms [25,26]. The electrochemical reduction of the layer deposited by drop-casting is accompanied by a slight enhancement of the I_D/I_G ratio from 0.70 to 1.25, and a narrowing of the D and G peaks. These apparently contrasting results can be explained by the different nature of the D peak in GO and RGO: in the first case, the peak is associated with an increased number of sp^3 carbon atoms due to

chemical functionalization, and the latter peak is attributed to the structural defects (e.g. vacancies) in the carbon framework [25].

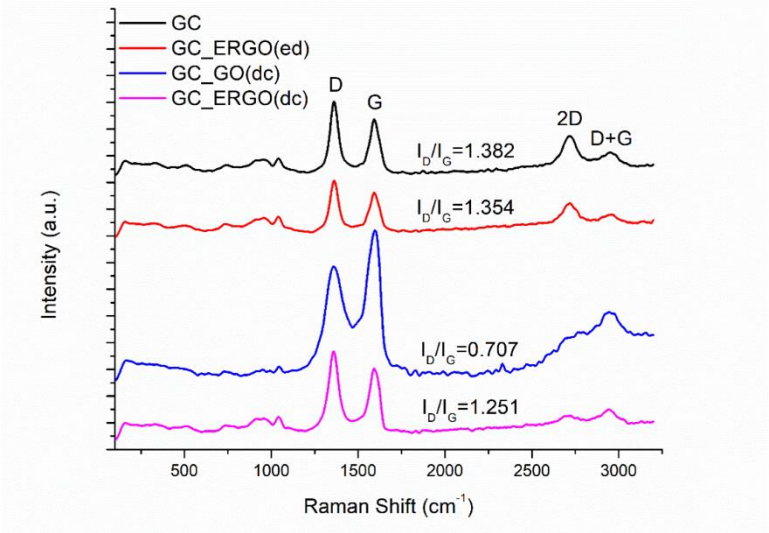

Fig. 6. Raman spectra of the bare GC substrate, and the modified electrodes GC_ERGO(ed), GC_GO(dc) and GC_ERGO(dc).

3.2.5. Electrochemical Characterization of Modified Electrodes

The determination of electrochemically active surface area (ECSA) for electrodes modified with nanomaterials proved to be experimentally challenging, and numerous researchers emphasized the limitations of the Randles-Ševčík equation when it comes to accurately determining the ECSA using CV experiments [27–30]. A rough evaluation of the thickness of the diffusion layer, in the commonly employed scan rates range (i.e. 0.02-0.1 Vs^{-1}) for the redox species employed in our study ($K_3[Fe(CN)_6]$ and ferrocene), indicates a value of several hundred micrometers, much larger than the expected surface roughness of our modified electrodes. It was established that under these conditions, the CV features are independent of the surface roughness, as the observed area corresponds to the projected area of the electrode surface [28,31]. Considering the above constraints, the Randles-Ševčík equation is applied here with the sole purpose of comparing the two preparation methods in terms of reproducibility, and not for obtaining precise ECSA values for the ERGO electrodes. In this context, a method similar to that developed by Bishop et al [32] was utilized for estimating the active surface area of ERGO electrodes, based on the voltammetric responses of two common redox probes: (a) 1 mM $K_3[Fe(CN)_6]$ in 0.1M KCl, and (b) 1mM ferrocene (Fc) in 0.1M $TBABF_4$, in MeCN.

The recorded CVs displayed a quasi-reversible shape, and thus the modified version of the Randles-Ševčík equation (1) has been considered [32–35]:

$$i_p = (2.69 \times 10^5) n^{3/2} A D^{1/2} C \nu^{1/2} K(\Lambda, \alpha) \quad (1)$$

where: i_p is the value of the oxidation peak current (expressed in A), *n* is the number of transferred electrons, A is the electrode surface area (cm^2), ν is the scan rate (Vs^{-1}), while *D*, and *C* represent the diffusion coefficient ($cm^2\ s^{-1}$), and the bulk concentration (mol cm^{-3}) of the redox species, respectively. The function *K*(Λ,α) depends on the kinetic parameter Λ, and the value of the electron transfer coefficient α (considered 0.5), and has it been determined using the method reported by Matsuda and Ayabe [36]. The kinetic parameter Λ defined as:

$$\Lambda = \pi^{1/2} \psi \quad (2)$$

can be calculated from the well-known theory developed by Nicholson for the application of CV in measurement of electrode reaction kinetics [37]. For the oxidized and the reduced forms of the employed redox probes, the following values of the diffusion coefficients have been reported in the literature: (a) $Fe(CN)_6^{3-}$: $D_R = 6.5\times10^{-6}\ cm^2\ s^{-1}$ [38], and (b) ferrocene: $D_O = 2.3\times10^{-5}\ cm^2\ s^{-1}$ [39,40].

The redox probes selected for this study display different kinetic sensitivity towards the surface chemistry of carbon electrodes [41]. The results obtained by employing the outer-sphere Fc/Fc^+ redox species indicate a higher area for the ERGO electrodes, and, as expected, this increase is more significant for GC_ERGO(dc) (Fig. 7). This is in agreement with the findings described in the previous section that revealed a higher roughness for the electrodes prepared by drop-casting procedure, which is a clear indication for a larger total surface area. However, we emphasize once again that the values displayed in the graph below are only estimations. The data presented in Fig. 7 show a 17-fold increase in the relative standard deviation of the estimated surface area for drop-cast electrodes compared to those obtained via direct electrodeposition. Hence, a clear conclusion that we may extract from these findings is the superior reproducibility of the direct electrodeposition procedure for producing ERGO-modified electrodes.

The CV recorded in the presence of surface sensitive $Fe(CN)_6^{3-/4-}$ redox probes displayed higher capacitive currents for ERGO than that of the bare GC electrodes, as it is expected for electrodes with larger electrochemically active surface area (results not shown). However, we observed an increase in the irreversibility of the voltammetric response after several minutes, in comparison with the curves registered immediately after preparing the electrodes (ΔE_p in the range 0.09 ÷0.16 V at scan rates of 20 Vs^{-1}). This is consistent with some previous observations which indicated that freshly prepared graphene is prone to surface contamination after short-time exposure to a typical laboratory atmosphere, that may hinder the electron transfer [42]. Moreover, it was suggested that for the inner-sphere species $Fe(CN)_6^{3-/4-}$, the electron transfer kinetics is also influenced by both the existence and charge state of the carboxylate functionalities on the ERGO surface [32]. Therefore, the results obtained in the presence of the outer-sphere

Fc/Fc^+ couple can be considered more reliable, as such systems are insensitive to surface chemistry and their kinetics is less influenced by the presence of surface oxides or nonspecific adsorbers [43].

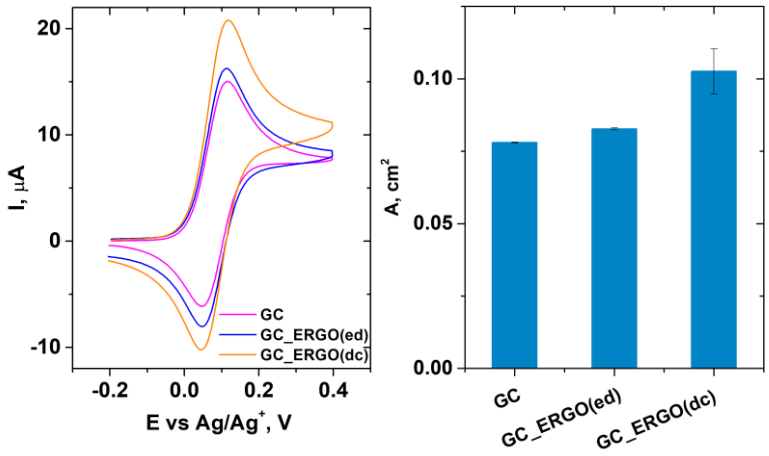

Fig. 7. (A) Cyclic voltammograms (100 mV s^{-1}) recorded in 1 mM ferrocene, 0.1 M TBATFB solution in MeCN, at GC and the ERGO electrodes prepared by the two procedures; (B) comparison of the estimated active surface area calculated with Randles-Ševčík equation in terms of reproducibility.

4. Conclusions

This work presents a comparative study regarding the morphology, surface chemistry, and electrochemical characteristics of ERGO-modified glassy carbon electrodes obtained by direct electrochemical deposition and electrochemical reduction of drop-casted GO. As far as we are aware, this is the first study that compares the two approaches, and it aims to underline the differences between the obtained ERGO-modified electrodes.

The XPS and Raman investigations indicated that both methods lead to ERGO deposits with similar surface chemistry. However, optical microscopy and AFM images showed that the surface of drop-casted electrodes is uniformly covered with a continuous ERGO layer, while through the direct electrochemical reduction of GO, isolated ERGO deposits are formed. Also, drop-casted electrodes have an increased surface roughness after the deposition of GO, which decreases considerably following the electrochemical reduction step. Finally, the voltammograms recorded in the presence of outer sphere redox couples indicated a slightly lower reproducibility in the case of the drop casting method.

Since ERGO-modified GC substrates are frequently used in the development of sensing devices, a comparative investigation of the commonly employed deposition methods is very useful. Although the integration of carbon

nanomaterials into the construction of sensors has clear advantages, ensuring the fabrication reproducibility is an essential requirement. Nonetheless, when deciding on the most appropriate deposition method, it's important to also consider the subsequent surface modification procedures employed for producing sensing devices.

Acknowledgements

This work was supported by a grant of the Romanian Ministry of Education and Research, CNCS—UEFISCDI, project number PN-III-P4-ID-PCE-2020-2474, within PNCDI III. AFM imaging was possible using infrastructure provided by the European Regional Development Fund through Competitiveness Operational Program 2014–2020, INNOVABIOMED (Project No. P_36_611).

R E F E R E N C E S

1. Serp, P. 7.13 - Carbon. In Comprehensive Inorganic Chemistry II (Second Edition): From Elements to Applications; Elsevier: Amsterdam, 2013; pp. 323–369 ISBN 978-0-08-096529-1.
2. Uskoković, V. A Historical Review of Glassy Carbon: Synthesis, Structure, Properties and Applications. Carbon Trends **2021**, 5, 100116, doi:https://doi.org/10.1016/j.cartre.2021.100116.
3. Zittel, H.E.; Miller, F.J. A Glassy-Carbon Electrode for Voltammetry. Anal. Chem. **1965**, 37, 200–203, doi:10.1021/ac60221a006.
4. Yoshimori, T.; Arakawa, M.; Takeuchi, T. Anodic Stripping Coulometry of Gold Using the Glassy Carbon Electrode. Talanta **1965**, 12, 147–152, doi:10.1016/0039-9140(65)80030-3.
5. Plock, C.E. Anodic Voltammetric Determination of Plutonium. Diffusion Coefficients of Putonium(III) in Mineral Acids. Anal. Chim. Acta **1970**, 49, 83–87, doi:10.1016/S0003-2670(01)80010-6.
6. Abdel-Aziz, A.M.; Hassan, H.H.; Badr, I.H.A. Glassy Carbon Electrode Electromodification in the Presence of Organic Monomers: Electropolymerization versus Activation. Anal. Chem. **2020**, 92, 7947–7954, doi:10.1021/acs.analchem.0c01337.
7. Marsili, E.; Rollefson, J.B.; Baron, D.B.; Hozalski, R.M.; Bond, D.R. Microbial Biofilm Voltammetry: Direct Electrochemical Characterization of Catalytic Electrode-Attached Biofilms. Appl. Environ. Microbiol. **2008**, 74, 7329–7337, doi:10.1128/AEM.00177-08.
8. Amouzadeh Tabrizi, M.; Shamsipur, M. A Label-Free Electrochemical DNA Biosensor Based on Covalent Immobilization of Salmonella DNA Sequences on the Nanoporous Glassy Carbon Electrode. Biosens. Bioelectron. **2015**, 69, 100–105, doi:10.1016/j.bios.2015.02.024.
9. Lakhera, P.; Chaudhary, V.; Jha, A.; Singh, R.; Kush, P.; Kumar, P. Recent Developments and Fabrication of the Different Electrochemical Biosensors Based on Modified Screen Printed and Glassy Carbon Electrodes for the Early Diagnosis of Diverse Breast Cancer Biomarkers. Mater. Today Chem. **2022**, 26, 101129, doi:https://doi.org/10.1016/j.mtchem.2022.101129.
10. Nimbalkar, S.; Fuhrer, E.; Silva, P.; Nguyen, T.; Sereno, M.; Kassegne, S.; Korvink, J. Glassy Carbon Microelectrodes Minimize Induced Voltages, Mechanical Vibrations, and Artifacts in Magnetic Resonance Imaging. Microsystems Nanoeng. **2019**, 5, doi:10.1038/s41378-019-0106-x.

11. Zhu, Z. An Overview of Carbon Nanotubes and Graphene for Biosensing Applications. Nano-Micro Lett. **2017**, 9, 1–24, doi:10.1007/s40820-017-0128-6.
12. Vlăsceanu, G.M.; Amărandi, R.M.; Ioniță, M.; Tite, T.; Iovu, H.; Pilan, L.; Burns, J.S. Versatile Graphene Biosensors for Enhancing Human Cell Therapy. Biosens. Bioelectron. **2018**, 117, 283–302, doi:10.1016/j.bios.2018.04.053.
13. Ioniţă, M.; Vlăsceanu, G.M.; Watzlawek, A.A.; Voicu, S.I.; Burns, J.S.; Iovu, H. Graphene and Functionalized Graphene: Extraordinary Prospects for Nanobiocomposite Materials. Compos. Part B Eng. **2017**, 121, 34–57, doi:10.1016/j.compositesb.2017.03.031.
14. Chiticaru, E.A.E.A.; Pilan, L.; Damian, C.M.C.-M.; Vasile, E.; Burns, J.S.J.S.; Ionita, M. Influence of Graphene Oxide Concentration When Fabricating an Electrochemical Biosensor for DNA Detection. Biosensors **2019**, 9, 1–18, doi:10.3390/bios9040113.
15. Chiticaru, E.A.; Ionita, M. Graphene Toxicity and Future Perspectives in Healthcare and Biomedicine. FlatChem **2022**, 35, 100417, doi:https://doi.org/10.1016/j.flatc.2022.100417.
16. Zhou, A.; Bai, J.; Hong, W.; Bai, H. Electrochemically Reduced Graphene Oxide: Preparation, Composites, and Applications. Carbon N. Y. **2022**, 191, 301–332, doi:https://doi.org/10.1016/j.carbon.2022.01.056.
17. Kim Thuong Nguyen, T.; Huong Giang Le, T.; Thi Thanh Pham, N.; Hoa Hoang, T.; Phuong Nguyen, H.; Xuan Nguyen, M.; Huong Giang Dang, M.; Hoang Do, H.; Thao Ta, T.; Thanh Bui, X. Development of Stripping Voltammetry Using Glassy Carbon Electrode Modified with Electrochemical Reduced Graphene Oxide for the Determination of Amaranth in Soft Drink and Candy Samples. Microchem. J. **2023**, 189, 108467, doi:https://doi.org/10.1016/j.microc.2023.108467.
18. Chen, L.; Tang, Y.; Wang, K.; Liu, C.; Luo, S. Direct Electrodeposition of Reduced Graphene Oxide on Glassy Carbon Electrode and Its Electrochemical Application. Electrochem. commun. **2011**, 13, 133–137, doi:10.1016/j.elecom.2010.11.033.
19. Guo, H.; Wang, X.; Qian, Q.; Wang, F.; Xia, X. A Green Approach to the Synthesis of Graphene Nanosheets. ACS Nano **2009**, 3, 2653–2659, doi:10.1021/nn900227d.
20. Du, D.; Guo, S.; Tang, L.; Ning, Y.; Yao, Q.; Zhang, G.J. Graphene-Modified Electrode for DNA Detection via PNA-DNA Hybridization. Sensors Actuators, B Chem. **2013**, 186, 563–570, doi:10.1016/j.snb.2013.06.045.
21. Devadas, B.; Rajkumar, M.; Chen, S.M.; Saraswathi, R. Electrochemically Reduced Graphene Oxide/ Neodymium Hexacyanoferrate Modified Electrodes for the Electrochemical Detection of Paracetomol. Int. J. Electrochem. Sci. **2012**, 7, 3339–3349, doi:10.1007/s10800-007-9392-3.
22. Chen, Y.; Xie, B.; Ren, Y.; Yu, M.; Qu, Y.; Xie, T.; Zhang, Y.; Wu, Y. Designed Nitrogen Doping of Few-Layer Graphene Functionalized by Selective Oxygenic Groups. Nanoscale Res. Lett. **2014**, 9, 1–8, doi:10.1186/1556-276X-9-646.
23. Jurkiewicz, K.; Pawlyta, M.; Zygadło, D.; Chrobak, D.; Duber, S.; Wrzalik, R.; Ratuszna, A.; Burian, A. Evolution of Glassy Carbon under Heat Treatment: Correlation Structure–mechanical Properties. J. Mater. Sci. **2018**, 53, 3509–3523, doi:10.1007/s10853-017-1753-7.
24. Jungen, A. Nano-Spectroscopy of Individual Carbon Nanotubes and Isolated Graphene Sheets. In Springer Series in Optical Sciences; 2011; Vol. 158, pp. 91–109.
25. Dimiev, A.M.; Eigler, S. Graphene Oxide: Fundamentals and Applications; 2016; ISBN 9781119069447.
26. Bîru, E.I.; Iovu, H. Graphene Nanocomposites Studied by Raman Spectroscopy. In; Nascimento, G.M. do, Ed.; IntechOpen: Rijeka, 2018; p. Ch. 9 ISBN 978-1-78923-001-7.
27. Davies, T.J.; Moore, R.R.; Banks, C.E.; Compton, R.G. The Cyclic Voltammetric Response of Electrochemically Heterogeneous Surfaces. J. Electroanal. Chem. **2004**, 574, 123–152, doi:10.1016/j.jelechem.2004.07.031.

28. Compton, R.G.; Batchelor-McAuley, C.; Dickinson, E.J.F. Understanding Voltammetry; 2011; ISBN 9781848167308.
29. Paixão, T.R.L.C. Measuring Electrochemical Surface Area of Nanomaterials versus the Randles−Ševčík Equation. ChemElectroChem **2020**, 7, 3414–3415, doi:10.1002/celc.202000633.
30. Ferrari, A.G.M.; Foster, C.W.; Kelly, P.J.; Brownson, D.A.C.; Banks, C.E. Determination of the Electrochemical Area of Screen-Printed Electrochemical Sensing Platforms. Biosensors **2018**, 8, 1–10, doi:10.3390/bios8020053.
31. Menshykau, D.; Streeter, I.; Compton, R.G. Influence of Electrode Roughness on Cyclic Voltammetry. J. Phys. Chem. C **2008**, 112, 14428–14438, doi:10.1021/jp8047423.
32. Bishop, G.W.; Ahiadu, B.K.; Smith, J.L.; Patterson, J.D. Use of Redox Probes for Characterization of Layer-by-Layer Gold Nanoparticle-Modified Screen-Printed Carbon Electrodes. J. Electrochem. Soc. **2017**, 164, B23–B28, doi:10.1149/2.0431702jes.
33. Washe, A.P.; Lozano-Sánchez, P.; Bejarano-Nosas, D.; Katakis, I. Facile and Versatile Approaches to Enhancing Electrochemical Performance of Screen Printed Electrodes. Electrochim. Acta **2013**, 91, 166–172, doi:10.1016/j.electacta.2012.12.110.
34. Bard, A.J.; Faulkner, L.R. ELECTROCHEMICAL METHODS Fundamentals and Applications; 2nd ed.; John Wiley & Sons, Inc., 2001; ISBN 0-471-04372-9.
35. Matei D. Raicopol, Andreea M. Pandele, Constanta Dascălu, E.V.; Anamaria Hanganu, Gabriela-Geanina Vasile, Ioana Georgiana Bugean, C.P.; Gabriela Stanciu, G.-O.B. Improving the Voltammetric Determination of Hg(II): A Comparison Between Ligand-Modified Glassy Carbon and Electrochemically Reduced Graphene Oxide Electrodes. Sensors **2020**, 20, 1–18.
36. Matsuda, H.; Ayabe, Y. Zur Theorie Der Randles-Sevčikschen Kathodenstrahl-Polarographie. Zeitschrift für Elektrochemie, Berichte der Bunsengesellschaft für Phys. Chemie **1955**, 59, 494–503, doi:10.1002/bbpc.19550590605.
37. Nicholson, R.S. Theory and Application of Cyclic Voltammetry for Measurement of Electrode Reaction Kinetics. Anal. Chem. **1965**, 37, 1351–1355, doi:10.1021/ac60230a016.
38. Cumba, L.R.; Foster, C.W.; Brownson, D.A.C.; Smith, J.P.; Iniesta, J.; Thakur, B.; Do Carmo, D.R.; Banks, C.E. Can the Mechanical Activation (Polishing) of Screen-Printed Electrodes Enhance Their Electroanalytical Response? Analyst **2016**, 141, 2791–2799, doi:10.1039/c6an00167j.
39. Wang, Y.; Rogers, E.I.; Compton, R.G. The Measurement of the Diffusion Coefficients of Ferrocene and Ferrocenium and Their Temperature Dependence in Acetonitrile Using Double Potential Step Microdisk Electrode Chronoamperometry. J. Electroanal. Chem. **2010**, 648, 15–19, doi:10.1016/j.jelechem.2010.07.006.
40. Sharp, M. Determination of The Charge-Transfer Kinetics of Ferrocene at Platinum and Vitreous Carbon Electrodes by Potential Step and Chronocoulometry. Electrochim. Acta **1983**, 28, 301–308, doi:10.1016/0013-4686(83)85126-3.
41. McCreery, R.L. Advanced Carbon Electrode Materials for Molecular Electrochemistry. Chem. Rev. **2008**, 108, 2646–2687, doi:10.1021/cr068076m.
42. Lounasvuori, M.M.; Rosillo-Lopez, M.; Salzmann, C.G.; Caruana, D.J.; Holt, K.B. Electrochemical Characterisation of Graphene Nanoflakes with Functionalised Edges. Faraday Discuss. **2014**, 172, 293–310, doi:10.1039/c4fd00034j.
43. Chen, P.; Fryling, M.A.; McCreery, R.L. Electron Transfer Kinetics at Modified Carbon Electrode Surfaces: The Role of Specific Surface Site. Anal. Chem. **1995**, 67, 3115–3122, doi:10.1021/ac00114a004.